RESEARCH PAPER

Thermodynamic Modeling of Wax Formation Temperature in Paraffinic Systems Using Cubic Plus Chain Equation of State

Ramin Jamali, Amir Abbas Izadpanah*, Hossein Rahideh

Department of Chemical Engineering, Faculty of Oil, Gas and Petrochemical Engineering, Persian Gulf University, Bushehr, P.O. Box 7516913817, Iran

ARTICLE INFO

Article History:
Received 27 November 2024
Revised 20 March 2025
Accepted 23 March 2025

Keywords:
CPC equation of state
Wax formation temperature
Multi-solid
Solid solution

ABSTRACT

The purpose of this research was to develop a thermodynamic model for predicting wax formation temperature, using the cubic plus chain (CPC) equation of state and multi-solid and solid solution models. The investigated systems in this work were binary and ternary systems of normal alkanes. In the solid solution model, the solid phase is considered as an ideal solution. In this research, the modeling results of wax formation temperature for six hydrocarbon systems were obtained and compared with experimental data. The hydrocarbon systems consisted of three ternary systems including C14-C15-C16, C16-C17-C18, C18-C19-C20 and also three binary systems including C14-C16, C17-C19, and C16-C18 systems. According to the obtained results, the average absolute error in calculating the wax formation temperature for these systems was 1.03% for the solid solution model and 0.67% for the multi-solid model. According to the average absolute error for these systems, it was found that the multi-solid model provided better results than the solid solution model. By comparing the obtained results, using the CPC and SRK equations of state, it was determined that the results of these two equations of state for these normal alkanes were almost similar. Comparing the results obtained in this work with the works of Parsa et al., Ghanaei et al., Shahahmadi et al., and Mansoorpour et al., showed that the accuracy of this model was comparable and noteworthy to these models and provided better results than some of these models.

How to cite this article
Jamali R, Izadpanah AA, Hossein Rahideh H., Thermodynamic Modeling of Wax Formation Temperature in Paraffinic Systems Using Cubic Plus Chain Equation of State, Journal of Oil, Gas and Petrochemical Technology, 2025; 12(1): 1-17. DOI:10.22034/jogpt.2025.490790.1132.

1. INTRODUCTION

Wax precipitation poses significant challenges to the oil industry. It is manifested as solid deposits that can be formed in reservoirs, production facilities, and pipelines. This problem mainly arises when crude oil cools below its cloud point temperature as heat dissipates to the environment. Such precipitation is problematic as it may lead to increased pressure drops, higher energy demands, and the potential blockage of pipelines.

At room temperature (75°F) and atmospheric pressure, C1 through C4 exist in the gaseous state, nC5 to nC15 are in the liquid state, and normal

* *Corresponding Author Email: izadpanah@pgu.ac.ir*

alkanes with carbon chains longer than nC15 are found in the solid state [1].

The wax formation point is identified using two key terms: wax appearance temperature (WAT), also called the cloud point, and wax disappearance temperature (WDT). WAT refers to the temperature at which the first solid paraffin crystals emerge as the solution cools. The wax appearance point depends on the crystallization kinetics of paraffins and can be influenced by factors such as cooling rate and detection methods, including microscopic observation, differential scanning calorimetry, laser-based solid particle detection, and viscometry [2, 3]. However, WDT refers to the threshold temperature where all solid wax crystals become entirely dissolved in the solution. It is important to note that the WAT may not always represent the thermodynamic equilibrium temperature, whereas the WDT corresponds to the equilibrium temperature between the solid and liquid phases [4].

At present, there are two primary approaches to thermodynamic modeling of wax formation equilibrium conditions. The first is the solid solution approach, where the solid phase is treated as a multi-component solution, containing all precipitating species within the same solid phase [5]. The second method, called multi-solid, assumes that each component forms its own pure solid phase when precipitating [6]. Each approach employs a distinct algorithm to calculate the equilibrium conditions for wax formation. In the solid solution perspective, the liquid phase is described by using either an equation of state with a suitable mixing rule or activity coefficient models. For the solid phase, fugacity is typically calculated using activity coefficient models. The multi-solid framework, in contrast, utilizes an EoS with mixing rules or activity coefficient models for the liquid phase. Given its assumption of pure-component solid phases, however, only pure solid fugacity is required to represent solid-phase behavior.

Won [7] pioneered one of the first solid solution approaches for modeling wax precipitation phenomena. The study presented a thermodynamic framework for analyzing vapor-liquid-solid phase equilibria in paraffinic hydrocarbon mixtures. Regular solution theory was utilized to model liquid-solid equilibria, while the Soave-Redlich-Kwong (SRK) equation of state (EoS) [8] was employed for vapor-liquid equilibria. Additionally, Won introduced a three-phase equilibrium calculation method and correlated fusion temperature and enthalpy of pure n-alkanes as functions of their molecular weights.

Pedersen et al., [9] enhanced Won's model for predicting WAT by calculating the activity coefficients for both solid and liquid phases using an improved version of regular solution theory.

Coutinho and Stenby [10] initially applied Wilson's model [11] to study the orthorhombic solid phase. Subsequently, Coutinho [12] proposed an adapted UNIQUAC model [13] to better describe this phase in solid-liquid equilibria for hydrocarbon mixtures. The UNIQUAC model [13] proved more versatile than Wilson's approach [11]. Furthermore, Coutinho investigated integrating UNIFAC with Flory's free-volume theory to address non-idealities in the liquid phase.

Ji et al., [4] established a solid solution model for WDT and wax precipitation analysis, combining UNIQUAC for solid-liquid equilibria with modified SRK/PR EoS [8, 14] for vapor-liquid equilibria. The model enhances accuracy through new heat capacity/fusion correlations considering n-alkane carbon number parity. Experimental validation was performed by measuring WDTs in certain binary systems to support the reliability of the proposed correlations.

Using multiple activity coefficient models, Esmaeilzadeh et al. [15] predicted WAT across various systems. For consecutive carbon numbers, the solid solution model [7] outperformed the multi-solid approach [6], which consistently underpredicted experimental WAT values.

Aftab et al., [16] experimentally measured the WDTs of two ternary systems C11-C16-C18 and C14-C16-C18 using a visual observation method. For thermodynamic modeling, they tested two solid solution approaches: *PCSAFT EoS* [17] for

the liquid phase combined with the *p.UNIQUAC model* [12] for solid-phase non-idealities, and an alternative method treating both phases with independent activity coefficient models. Their results demonstrated that the most precise predictions were achieved sing *regular solution theory* [5] for the liquid phase and the *predictive Wilson model (p.Wilson)* [10] for the solid phase.

Parsa et al., [18] conducted experiments to measure the WDTs of the three binary mixtures: C11-C18, C16-C18, and C14-C16. They compared the experimental results with predictions from thermodynamic models based on solid-solution theory. For the C11-C18 and C16-C18 systems, the combination of liquid-phase ideal solution theory and solid-phase p.UNIQUAC [12] yielded the most precise predictions. In contrast, the C14-C16 system achieved the best agreement using ideal solution theory combined with the p.Wilson model [10].

Nasrifar and Fani Kheshty [19] used a modified predictive UNIQUAC model by Ghanaei et al., [20], which included a pressure-dependent term based on the Clapeyron equation, and a generalized heat capacity correlation for liquid, disordered, and ordered solid phases to estimate the WDT and wax content in diverse hydrocarbon mixtures.

Building on solid solution theory, Bagherinia et al., [21] formulated a thermodynamic model combining PC-SAFT EoS (vapor-liquid phases) and UNIQUAC (solid phase) for WAT estimation. Validation using six North Sea crude samples confirmed its predictive accuracy for the wax precipitation.

A newly modified regular solution model formed the basis of Yang et al., [22] new thermodynamic approach to wax precipitation prediction. Their approach was solid solution method. Their model predicted WAT and solid precipitation curve with a good accuracy.

Nikolaidis et al., [23] developed a thermodynamic model for methane-n-alkane phase equilibria, employing volume-translated cubic EoS to improve Poynting correction accuracy. The results closely matched experimental data, including high-pressure conditions.

Wang et al., [24] proposed an NRTL-based model for n-alkane solid-liquid equilibrium that handled ordered solid phase non-ideality and generated transition phase diagrams for complete/ partial miscibility scenarios.

Shariatrad et al., [25] measured WDTs for a quaternary n-alkane system and compared them with a predictive solid solution model. Among the tested approaches, the combination of predictive UNIQUAC (solid) and regular solution theory (liquid) showed the best agreement.

Lira Galina et al., [6] pioneered the first multi-solid phase modeling approach for the wax precipitation. Their thermodynamic framework enabled wax deposition calculations across broad temperature ranges in petroleum systems, employing an equation of state for liquid-phase property determination. The model demonstrated strong correlation with experimental data for both binary and multicomponent hydrocarbon systems, including crude oil mixtures.

Nichita et al., [26] presented a modified multi-solid model to predict gas-solid behavior in binary mixtures of heavy alkanes, methane and carbon dioxide. In the following, the phenomenon of retrograde condensation for the wax phase in gas condensate systems is discussed, followed by the effect of pressure on the wax precipitation. Then a comparison of solid solution (SS) and multi-solid (MS) models was also made. Their results showed that the modified model of the solubility of heavy n-alkanes in methane and carbon dioxide is in good agreement with the experimental data for the three synthetic mixtures. The amount of the precipitated wax showed the interesting phenomenon of reverse condensation in gas condensates, which was similar to the phenomenon of reverse condensation in gas-liquid systems. By reducing the pressure, first an increase in the amount of wax, then a decrease and then an increase in the amount of wax in the three-phase mixture of wax-liquid-gas was observed.

Delirsefat et al., [27] created a multi-solid-based model using modified Peng-Robinson

(MPR) EoS for phase equilibria and innovative solid-fugacity determination. This computational tool accurately predicted WAT and wax amounts in North Sea oils, matching experimental data.

The perturbed hard sphere chain (PHSC) EoS [29, 30]]-based multi-solid model by Shaahmadi et al., [28] achieved accurate WDT predictions for n-alkane mixtures, performing comparably to experimental data and activity coefficient approaches.

Bazoyar et al., [31] developed a predictive model for determining wax formation temperature and precipitated wax quantity in normal alkanes. Their approach combined the perturbed hard sphere chain equation of state (PHSC EoS) with the multi-solid model. The results demonstrated superior performance compared to solid solution theory, with predictions for both wax formation temperature and precipitated wax amount aligning more closely with the experimental data for certain n-alkane mixtures.

Escobar-Remolina [32] introduced a predictive model designed to assess paraffinic wax precipitation. Built upon concepts of ideality, thermodynamic stability, and multi-solid precipitation within an EoS framework, this model demonstrated strong alignment with experimental data. Its outcomes frequently surpassed or matched the accuracy of previous models.

Vahabzadeh Asbaghi et al., [33] developed a Paraffin, Naphthene, and Aromatic (PNA)-based predictive method for petroleum fractions, combining sequential multi-solid modeling with perturbed chain statistical associating fluid theory (PC-SAFT) EoS and tuned binary interaction coefficients (BICs) for accurate wax/WAT predictions. The proposed model was tested using six crude oils from the North Sea, analyzing the role of different hydrocarbon families in precipitation. The results showed significant improvements over the previous models, with a minimal error in WAT predictions compared to the experimental data.

Vahabzadeh Asbaghi et al., [34] developed a composition-based classification system for wax modeling, combining PC-SAFT/multi-solid theory with the parameter optimization. Their 15-pseudo-component approach (MW ≤ 1200) accurately predicted WAT and wax content in high-wax crudes.

Accurate prediction of wax formation temperatures and deposition quantities fundamentally depends on reliable thermophysical properties of n-alkanes. Addressing this need, Alhejaili et al., [35] conducted systematic measurements for pure n-alkanes (C17-C50) using micro differential scanning calorimetry. Their study revealed that while fusion temperatures can be reliably estimated through simple carbon-number correlations, existing models showed significant deficiencies in predicting enthalpy of fusion and solid-solid transition enthalpies. To overcome these limitations, the researchers implemented corrective formulations for fusion enthalpies and established novel correlation schemes for the solid-phase transition enthalpies.

In addition to thermodynamic modeling to calculate wax formation temperature, which was discussed, other methods such as machine learning, etc. have also been used to calculate and predict wax formation temperature.

Amiri-Ramsheh et al., [36] compared six machine learning (ML) models (RBF, MLP, ANFIS, RF, ET, DT) for WDT prediction, identifying Random Forest as the most accurate. Results confirmed positive WDT correlations with the pressure and molecular weight.

Nait Amar et al. [37] introduced a machine learning-based approach, gene expression programming (GEP), to develop a smart correlation for accurately predicting WDT. Comprehensive experimental data support the correlation's high accuracy, with statistical metrics showing excellent performance. The GEP-based correlations outperform many existing methods, offering physical validity and consistency. These findings enhance WDT estimation, aiding in the simulation of wax deposition phenomena.

Wang and Chen [38] 's co-crystal-inclusive thermodynamic model, incorporating Flory-Huggins theory and lamellar structure, accurately

predicted low-pressure WAT and temperature-dependent wax precipitation in paraffin mixtures.

According to the literature review, it can be seen that to calculate or predict the wax formation temperature, various equations of state such as cubic equations of state, PC-SAFT, PHCT, etc. have been used in the multi-solid model. Using these equations of state in some models and systems has improved the results.

The CPC molecular model offered a more accurate depiction of chain-like molecules, including n-alkanes and polymers. When applied to phase behavior modeling, the CPC equation of state demonstrated significant advancements over the traditional cubic equation of state, primarily because of its enhanced molecular representation [39, 40].

This study aimed to predict wax formation temperatures in binary and ternary n-alkane systems using the CPC EoS combined with both multi-solid and solid solution approaches. The methodology employed the CPC EoS exclusively for determining liquid-phase thermodynamic properties (component fugacities), while treating the solid phase as an ideal solution in the solid solution model framework.

2. Modeling

2.1. Thermodynamic modeling of wax formation conditions

Modeling wax formation conditions requires establishing thermodynamic equilibrium among the coexisting phases. This equilibrium condition is mathematically expressed through component fugacity equality across all phases. If the existing phases are liquid and solid, we will have:

$$\hat{f}_i^L(T,P,x) = \hat{f}_i^S(T,P,s) \tag{1}$$

Equation (1) defines f as component fugacity, with T (temperature), P (pressure), x (liquid-phase composition), and s (solid-phase composition) as system variables. The liquid-phase fugacity term is derivable through equations of state. In this work, the CPC EoS [28 and 29] is used.

$$\hat{f}_i^L(T,P,x) = x_i\ \hat{\varphi}_i^L(T,P,x)\ P \tag{2}$$

equation (2) incorporates: x_i: liquid-phase mole fraction of component i, $\hat{\varphi}_i^L$: liquid-phase fugacity coefficient of component i. For the solid phase, component fugacity is typically characterized through activity coefficients:

$$\hat{f}_i^S(T,P,s) = s_i\ \gamma_i^S(T,P,s)\ f_i^{0S}(T,P) \tag{3}$$

In equation (3), s_i and γ_i^S respectively denote the solid-phase mole fraction and activity coefficient of component i, while f_i^{0S} represents its standard-state fugacity at system temperature and pressure - typically approximated by the pure component solid fugacity $f_{pure,i}^S$. under identical conditions.

$$f_i^{0S}(T,P) = f_{pure,i}^S(T,P) \tag{4}$$

An ideal solution approximation is applied to the solid phase in this work, therefore $\gamma_i^S(T,P,s)=1$, then

$$\hat{f}_i^S(T,P,s) = s_i\ f_{pure,i}^S(T,P) \tag{5}$$

$f_{pure,i}^S$ is calculated from the fugacity ratio $f_{pure,i}^L/f_{pure,i}^S$.

$$f_{pure,i}^S(P,T) = f_{pure,i}^L(P,T) * \exp\left[\frac{\Delta h_i^f}{R\,T_i^f}\left(1-\frac{T}{T_i^f}\right)+\frac{\Delta C_{pi}}{R}\left(1-\frac{T_i^f}{T}\right)-\frac{\Delta C_{pi}}{R}\left(ln\frac{T_i^f}{T}\right)+\int_{p0}^{P}\frac{\Delta v_i^S}{RT}dP\right] \tag{6}$$

equation (6) incorporates the following thermodynamic properties for pure component i: Δh_i^f is the fusion enthalpy, T_i^f is the fusion temperature, ΔC_{pi} is the heat capacity difference between liquid and solid phases and Δv_i^S is the molar volume difference between liquid and solid phases. An equation of state can be used to obtain $f_{pure,i}^L$. If solid-state transition is considered:

$$f_{pure,i}^S(P,T) = f_{pure,i}^L(P,T) * \exp\left[\frac{\Delta h_i^f}{RT_i^f}\left(1-\frac{T}{T_i^f}\right)+\frac{\Delta h_i^{tr}}{RT_i^{tr}}\left(1-\frac{T}{T_i^{tr}}\right)+\frac{\Delta C_{pi}}{R}\left(1-\frac{T_i^f}{T}\right)-\frac{\Delta C_{pi}}{R}\left(ln\frac{T_i^f}{T}\right)+\int_{p0}^{P}\frac{\Delta v_i^S}{RT}dP\right] \tag{7}$$

Where, Δh_i^{tr} is enthalpy change during solid-state phase transition and T_i^{tr} is the solid-state transition temperature.

2.2. Fusion and solid-state transitions properties

To calculate pure solid fugacity, as seen from equation (6), melting properties and transition solid-state properties are needed. The equations (8) to (23) have been used for the melting and solid- state transition properties [4].

2.2.1. Melting point:

For normal paraffins with an odd number of carbon atoms, $C_9 < C_n \leq C_{43}$

$$T_i^f(K) = 0.0122\, C_n^2 - 2.0861 C_n - \frac{775.598}{C_n} + 76.2189\, ln(C_n) + 156.9 \quad (8)$$

For normal paraffins with an even number of carbon atoms, $C_{10} < C_n \leq C_{42}$

$$T_i^f(K) = 0.0031\, C_n^3 - 0.3458 C_n^2 + 14.277 C_n + 137.73 \quad (9)$$

for $C_n > C_{42}$

$$T_i^f(K) = \frac{414.3(C_n - 1.5)}{C_n + 5} \quad (10)$$

solid state transition temperature for odd-carbon-number n-alkanes, $C_9 < C_n \leq C_{43}$

$$T_i^{tr}(K) = 0.0039\, C_n^3 - 0.4239\, C_n^2 + 17.28 C_n - ln(C_n) + 95.4 \quad (11)$$

solid state transition temperature for even -carbon-number n-alkanes, $C_{22} < C_n \leq C_{42}$

$$T_i^{tr}(K) = 0.0032\, C_n^3 - 0.3249\, C_n^2 + 12.78 C_n + ln(C_n) + 154.19 \quad (12)$$

2.2.2. The sum of melting enthalpy and solid-state transition enthalpy:

For odd-carbon-numbered n-alkanes:

$$h_{sum}(cal\ mol^{-1}) = 0.119\ MW * \mathrm{T}^f + 672.2, \quad for\ C_n \leq C_9 \quad (13)$$

$$h_{sum}(cal\ mol^{-1}) = 0.167\ MW * \mathrm{T}^f + 432.47, \quad for\ C_9 < C_n \leq C_{33} \quad (14)$$

$$h_{sum}(cal\ mol^{-1}) = 0.139\ MW * \mathrm{T}^f + 3984.8, \quad for\ C_n > C_{33} \quad (15)$$

For even -carbon-numbered n-alkanes

$$h_{sum}(cal\ mol^{-1}) = 0.180\ MW * \mathrm{T}^f + 522.7, \quad for\ C_n \leq C_{34} \quad (16)$$

$$h_{sum}(cal\ mol^{-1}) = 0.139\ MW * \mathrm{T}^f + 3984.8, \quad for\ C_n > C_{34} \quad (17)$$

2.2.3. Melting enthalpy and solid-state transition enthalpy:

For odd-carbon-numbered n-alkanes:

$$\Delta h^f(cal\ mol^{-1}) = 1.0\ \Delta H_{sum}, \quad \Delta h^{tr}(cal\ mol^{-1}) = 0.0 \quad for\ C_n \leq C_9 \quad (18)$$

$$\Delta h^f(cal\ mol^{-1}) = 0.74\ \Delta H_{sum}, \quad \Delta h^{tr}(cal\ mol^{-1}) = 0.26\ \Delta H_{sum}, \quad for\ C_9 < C_n \leq C_{43} \quad (19)$$

$$\Delta h^f(cal\ mol^{-1}) = 1.0\ \Delta H_{sum}, \quad \Delta h^{tr}(cal\ mol^{-1}) = 0.0, \quad for\ C_n > C_{43} \quad (20)$$

For even -carbon-numbered n-alkanes

$$\Delta h^f(cal\ mol^{-1}) = 1.0\ \Delta H_{sum}, \quad \Delta h^{tr}(cal\ mol^{-1}) = 0.0, \quad for\ C_n \leq C_{20} \quad (21)$$

$$\Delta h^f(cal\ mol^{-1}) = 0.64\ \Delta H_{sum}, \quad \Delta h^{tr}(cal\ mol^{-1}) = 0.36\ \Delta H_{sum}, \quad for\ C_{20} < C_n \leq C_{42} \quad (22)$$

$$\Delta h^f(cal\ mol^{-1}) = 1.0\ \Delta H_{sum}, \quad \Delta h^{tr}(cal\ mol^{-1}) = 0.0, \quad for\ C_n > C_{42} \quad (23)$$

2.2.4. Heat capacity

The solid-liquid heat capacity difference, ΔC_{pi} , was computed using the Pedersen et al., [8] correlation:

$$\Delta C_{pi} = 0.3033\ MW_i\ - 4.635 * 10^{-4}\ MW_i T \quad (24)$$

2.3. Solid solution and multi-solid models

Wax formation temperatures in the solid solution model are derived by solving liquid-solid fugacity equilibria (equation 1). Using only an EoS with ideal solid solution assumptions reduces these to equation (25):

$$x_i\ \hat{\varphi}_i^L(T,P,x)\ P = s_i\ f_{pure,i}^S(T,P) \quad (25)$$

$$k^{SL} = \frac{s_i}{x_i} = \frac{\hat{\varphi}_i^L(T,P,x)\ P}{f_{pure,i}^S(T,P)} \quad (26)$$

Given a defined liquid-phase composition, the wax formation temperature can be determined using computational methods analogous to bubble/dew point calculations in phase equilibria.

In the multi-solid model, using the equilibrium equation and phase stability analysis we will have equation (27).

$$\hat{f}_i^L(T,P,x) - f_{pure,i}^S(P,T) = 0 \qquad i = 1, \ldots\ldots, N \quad (27)$$

To obtain the temperature of wax formation, equation (27) must be solved for all components in the solution, and the highest temperature obtained is the temperature of wax formation.

2.4. CPC equation of state

This study employs the CPC EoS developed by Sisco et al., [28,29] to calculate liquid-phase component fugacity coefficients. The pressure-explicit form of the CPC EoS is expressed in Equation (28):

$$P_{CPC} = \frac{RT}{\upsilon}\left(1 + \frac{\overline{m}(\overline{m}b)}{\upsilon - \overline{m}b}\right) - \frac{\overline{m}^2 a}{\upsilon(\upsilon + \overline{m}b)} - \frac{RT}{\upsilon}\left(\frac{\overline{m}b}{\upsilon}\sum_{i=1}^{c} x_i(m_i - 1)\frac{0.475\upsilon}{\upsilon - 0.475\overline{m}b}\right) \quad (28)$$

In equation (28), υ is the molar volume, m is the number of segments in the molecule, b is the volume of the molecules or co-volume, and a represents the intermolecular attraction forces. The parameters a and b are the parameters of the Redlich- Kwong equation of state and are obtained from relations (29) to (31).

$$a_i = \Omega_{a_i}\left(m_i\right)\frac{R^2\ T_{c,i}^2}{P_{c,i}}\alpha \quad (29)$$

$$\alpha = \sqrt{\frac{T_c}{T}} \quad (30)$$

$$b_i = \Omega_{b_i}\left(m_i\right)\frac{R\ T_{c,i}}{P_{c,i}} \quad (31)$$

The parameters $\overline{m}$, $\overline{m}b$ and $\overline{m}^2 a$ are related to the mixture and are calculated through relations (32) to (35).

$$\overline{m} = \sum_{i=1}^{c} x_i\ m_i \quad (32)$$

$$\overline{m}\,b = \sum_{i=1}^{c} x_i\ m_i\ b_i \quad (33)$$

$$\overline{m}^2\ a = \sum_{i=1}^{c}\sum_{j=1}^{c} x_i\ x_j\ m_i\ m_j\ a_{ij} \quad (34)$$

$$a_{ij} = \sqrt{a_i\ a_j}\left(1 - k_{ij}\right) \quad (35)$$

Appendix A provides a comprehensive explanation of the equations associated with the CPC equation of state.

3. RESULTS AND DISCUSSION

The hydrocarbon systems used in this research included three ternary systems including C14-C15-C16, C16-C17-C18 and C18-C19-C20 systems, as well as three binary systems including C14-C16, C16-C18, and C17-C19.

A comparative analysis was conducted between

the CPC EoS and SRK EoS results. Modeling results were obtained for different systems at a single pressure of one bar. In all calculations, the binary interaction parameter, $k_{ij} = 0$ was considered.

The selected components in these systems and their molecular weight, critical properties and CPC segment number are presented in Table 1.

Table 1. Molecular weight, Critical Properties and Chain Lengths for Selected Paraffins in CPC EoS [30]

Component	MW [g/mol]	Tc [K]	Pc [bar]	m [-]
Undecane	156.312	639.0	19.50	6.2173
Tetradecane	198.392	693.0	15.70	8.0164
Pentadecane	212.419	708.0	14.80	8.7008
Hexadecane	226.446	723.0	14.0	9.1951
Heptadecane	240.473	736.0	13.40	10.0490
Octadecane	254.49	747.0	12.70	10.6229
Nonadecane	268.527	758.0	12.10	11.1571
eicosane	282.553	768.0	11.60	11.7654

Moreover, the values for the parameters $\Omega_a(m), \Omega_b(m)$ and Zc for all compounds used in this work were calculated with the CPC EoS and presented separately in Table 2.

Table 2. CPC EoS simulation parameters for n-alkanes calculated in this work

Component	$\mathbf{Z_c}$	$\boldsymbol{\Omega_a(m)}$	$\boldsymbol{\Omega_b(m)}$
C_{14}	0.335	0.0083	**0.0056**
C_{15}	0.335	0.0073	**0.0050**
C_{16}	0.335	0.0066	**0.0046**
C_{17}	0.335	0.0056	**0.0046**
C_{18}	0.335	0.0051	**0.0038**
C_{19}	0.335	0.0041	**0.0035**
C_{20}	0.335	0.0040	**0.0033**

Also, equation (34) is used to calculate the average absolute error (AAE%) of the wax formation temperature (WAT) resulting from this research and previous works in comparison with the exprimental data for different hydrocarbon mixtures:

$$AAE\% = \left(\frac{100}{n}\right)\sum_{i}^{n}\left|\frac{WAT_i^{cal} - WAT_i^{exp}}{WAT_i^{exp}}\right| \quad (36)$$

In equation (34), n is the total number of experimental data, (WAT_i^{cal}) is the calculated wax formation temperature using the model, and (WAT_i^{exp}) is the exprimental wax formation temperature.

For these ternary and binary systems, the wax formation temperature has been calculated using CPC and SRK equations of state and solid solution and multi-solid models. To compare the results obtained from these two equations of state and different models, the average absolute error was calculated and reported in Tables 3 to 8.

Table 3 shows the results related to system 1, which includes normal alkanes C14-C15-C16. As can be seen, the average absolute error is higher for the solid solution model than for the multi-solid model. It can also be seen that the accuracy of CPC and SRK equation of state in predicting wax formation temperature for this system is almost the same. There is no particular advantage in using the CPC over the SRK equation of state.

Table 3. Results of wax formation temperature obtained from the model for system 1, including C14-C15-C16

Mixture number	Mole fraction			EXP WAT (K)	Solid Solution		Multi-Soild	
	C14	C15	C16		CPC EoS WAT (K)	SRK EoS WAT (K)	CPC EoS WAT (K)	SRK EoS WAT (K)
1	0.06	0.57	0.37	283	287.4	288.1	280.2	285.6
2	0.14	0.23	0.63	285	288.5	288.6	288.1	288.1
3	0.17	0.06	0.77	286	289.2	289.3	289.1	289.1
4	0.24	0.33	0.43	282	287.2	287.4	286.3	286.3
5	0.21	0.56	0.23	281	285.8	285.8	283.3	283.4
6	0.27	0.66	0.07	280	283.6	283.6	280.9	280.9
7	0.37	0.05	0.58	283	287.7	287.9	287.6	287.7
8	0.32	0.24	0.44	282	287.3	287.4	286.5	287.8
9	0.43	0.33	0.24	279	285.0	285.4	283.6	283.6
10	0.57	0.17	0.26	278	284.3	285.3	283.4	284.0
11	0.73	0.14	0.13	276	283.4	283.3	280.7	280.8
AAE%					1.76	1.83	1.30	1.37

Table 4. The results of wax formation temperature obtained from the model for system 2, including C16-C17-C18

Mixture number	Mole fraction			EXP	Solid Solution		Multi-Soild	
	C16	C17	C18		CPC EoS	SRK EoS	CPC EoS	SRK EoS
1	0.1	0.1	0.8	298	299.7	299.8	299.8	299.9
2	0.1	0.75	0.15	294	293.8	293.8	296.3	296.5
3	0.1	0.8	0.1	295	294.2	294.1	296.0	296.0
4	0.11	0.39	0.5	296	297.5	297.3	298.6	298.5
5	0.2	0.2	0.6	296	298.2	298.0	299.0	299.1
6	0.2	0.6	0.2	294	293.7	293.6	296.5	296.6
7	0.33	0.33	0.34	293	295.7	295.6	297.4	297.4
8	0.4	0.1	0.5	294	297.3	297.2	298.2	298.1
9	0.4	0.4	0.2	292	293.5	293.6	295.8	296.2
10	0.6	0.2	0.2	291	293.7	293.6	295.7	295.7
11	0.8	0.1	0.1	290	290.8	290.7	293.9	293.9
Average AAE%					1.06	1.08	0.54	0.55

Table 5. The results of wax formation temperature obtained from the model for system 3, including C18-C19-C20

Mixture number	Mole fraction			EXP	Solid Solution		Multi-Soild	
	C18	C19	C20		CPC EoS	SRK EoS	CPC EoS	SRK EoS
1	0.02	0.02	0.96	309	309.7	309.6	309.6	309.6
2	0.05	0.05	0.9	309	309.4	309.4	309.7	309.3
3	0.05	0.9	0.05	305	305.5	305.5	304.6	304.7
4	0.1	0.1	0.8	308	309.1	309.1	308.7	308.8
5	0.1	0.4	0.5	306	307.8	307.9	306.9	306.8
6	0.1	0.55	0.35	306	307.2	307.2	305.3	305.3
7	0.14	0.73	0.13	304	305.9	305.9	303.7	303.8
8	0.15	0.15	0.7	307	308.7	308.7	308.2	308.3
9	0.2	0.2	0.6	306	308.9	308.2	307.5	307.6
10	0.2	0.6	0.2	305	306.2	306.4	305.3	304.0
11	0.26	0.26	0.48	306	307.6	307.6	306.5	306.8
12	0.33	0.33	0.34	304	306.9	306.7	305.1	305.2
13	0.4	0.1	0.5	305	307.5	307.3	306.8	306.9
14	0.43	0.43	0.14	303	305.2	305.2	301.4	301.5
15	0.48	0.15	0.37	304	306.6	306.8	305.4	305.4
16	0.6	0.2	0.2	302	305.3	305.3	303.0	303.1
17	0.79	0.11	0.1	301	303.6	303.7	300.3	303.3
18	0.9	0.05	0.05	301	302.5	302.5	300.4	297.5
AAE%					0.58	0.59	0.28	0.39

Table 6. Results of wax formation temperature obtained from the model for system 4, including C14-C16

Mixture number	Mole fraction		EXP	Solid Solution		Multi-Soild	
	C14	C16		CPC EoS	SRK EoS	CPC EoS	SRK EoS
1	1.0	0.0	279.4	278.3	278.3	278.3	278.3
2	1.0	0.0	278.7	278.1	280.1	278.2	278.2
3	0.9	0.1	277.3	281.9	281.9	279.2	279.2
4	0.9	0.1	275.9	282.8	282.8	280.7	280.7
5	0.7	0.3	277.6	285.2	285.3	284.2	284.2
6	0.6	0.4	280.2	285.9	285.9	285.8	285.9
7	0.5	0.5	284.3	287.8	287.8	287.5	287.5
8	0.3	0.7	288.3	289.0	289.0	288.8	288.8
9	0.1	0.9	290.3	289.8	289.8	289.8	289.7
10	0.0	1.0	291.5	290.3	290.3	290.3	290.3
AAE%				1.15	1.18	0.92	0.93

Table 7. Results of wax formation temperature obtained from the model for system 5, including C16-C18

Mixture number	Mole fraction		EXP	Solid Solution		Multi-Soild	
	C16	C18		CPC EoS	SRK EoS	CPC EoS	SRK EoS
1	1.0	0.0	291.5	290.3	290.3	290.3	290.3
2	0.9	0.1	289.7	293.5	293.5	290.8	290.7
3	0.8	0.2	290.4	295.0	294.9	293.3	293.2
4	0.7	0.3	292.0	296.7	296.6	295.8	295.7
5	0.5	0.5	293.9	297.9	297.8	297.3	297.1
6	0.5	0.5	293.5	297.9	297.9	297.4	297.3
7	0.3	0.7	296.4	299.1	299.1	298.8	298.8
8	0.2	0.8	299.4	299.8	299.9	299.7	299.8
9	0.1	0.9	300.6	300.3	300.3	300.3	300.3
10	0.0	1.0	301.6	300.7	300.8	300.8	300.8
Average AAE%				0.91	0.93	0.67	0.68

Table 8. Results of wax formation temperature obtained from the model for system 6, including C17-C19

Mixture number	Mole fraction		EXP	Solid Solution		Multi-Soild	
	C17	C19		CPC EoS	SRK EoS	CPC EoS	SRK EoS
1	0.99	0.002	295	295.8	295.3	295.2	295.2
2	0.94	0.05	295	297.0	297.0	295.1	295.0
3	0.84	0.16	295	299.2	299.2	297.2	297.3
4	0.75	0.25	297	300.3	300.4	299.1	299.1
5	0.49	0.51	300	302.4	302.5	299.8	300.0
6	0.25	0.75	302	304.1	303.5	303.9	300.5
7	0.1	0.89	303	304.7	304.8	304.7	304.7
8	0.002	0.99	305	305.2	305.2	305.3	305.2
AAE%				0.67	0.71	0.35	0.38

Results for systems 2-6 appear in Tables 4-8, showing consistently higher AAE for the solid solution compared to the multi-solid model.

The observed discrepancy in average absolute errors between models may stem from the ideal solution assumption applied to the solid phase in the solid solution approach. This simplification appears particularly problematic for n-alkanes, where the ideal solution hypothesis leads to the significant deviations between the predicted and experimental wax formation temperatures.

For better comparison, the results of calculating wax formation temperature using the model used in this work and the experimental data for system number 1, including C14-C15-C16, are shown in Figures 1 and 2. In Figures 1 and 2, the experimental data are marked with blue bars and the model-derived data are marked with gray and orange bars. Figure 1 shows the results of the solid solution model using the CPC and SRK equation of state. As shown, the accuracy of the CPC and SRK equations in calculating the wax formation

temperature for this system is close, and the solid solution model has calculated the wax formation temperature higher than the experimental value.

Analysis of Figure 2 reveals that in the multi-solid framework, CPC and SRK EoS yield nearly equivalent predictive accuracy and model outputs show improved correspondence with experimental data.

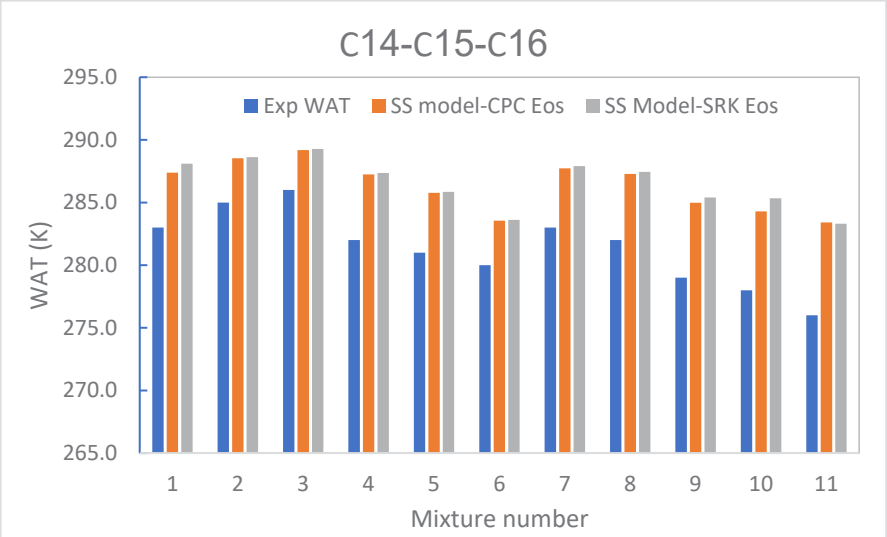

Figure 1. Comparison of the results obtained in calculating wax formation temperature of the system C14-C15-C16 using CPC and SRK equation of states and the solid solution model

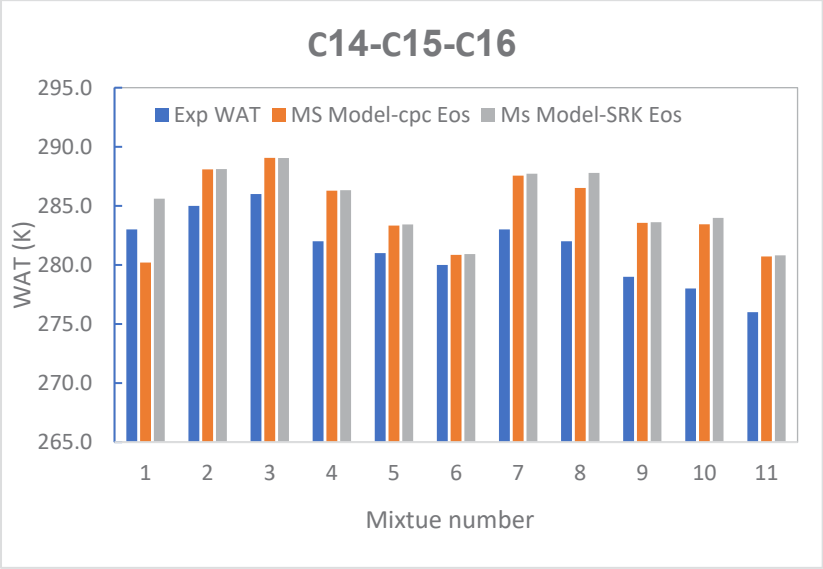

Figure 2. Comparison of the results obtained in calculating wax formation temperature of the system C14-C15-C16 using CPC and SRK equation of states and the multi-solid model

For comprehensive comparison, Table 9 summarizes the n-alkane system corresponding average absolute errors.

Table 10 compares the results of this work with other studies. Of course, this comparison has been made only according to the average absolute error. The average absolute error of other works is taken directly from the same work. As shown in Table 10, the CPC equation of state and multi-solid model produce results consistent with alternative models. Ghanai, Shah Ahmadi and Parsa models are non-ideal solid solution models. Compared with these three models, the results of this work using the CPC equation of state and the multi-solid model provided better results. Using the relationships related to melting properties can be another reason for the good results of the model presented in this study.

Using appropriate relationships for melting properties and considering solid state transition enthalpy and solid-state transition temperature can improve the prediction results of wax formation temperature.

Table 9. Comprehensive modeling results - system-specific and overall average absolute errors

System number	components	Solid Solution (AAE%)		Multi-Solid (AAE%)	
		CPC EoS	SRK EoS	CPC EoS	SRK EoS
1	C14-C15-C16	1.76	1.83	1.30	1.37
2	C16-C17-C18	1.06	1.08	0.54	0.55
3	C18-C19-C20	0.58	0.59	0.28	0.39
4	C14-C16	1.15	1.18	0.92	0.93
5	C16-C18	0.91	0.93	0.67	0.68
6	C17-C19	0.67	0.71	0.35	0.38
Average AAE%		1.03	1.06	0.67	0.71

Table 10. Accuracy comparison between present model and the existing approaches

System Number		1	2	3	4	5	6
Models AAE%	Ghanaei et al., [20]	0.62	0.77	0.84	0.16	-	-
	Mansourpoor et al., [41]	0.62	0.51	0.54	-	-	-
	Shaahmadi et al., [28]	0.49	0.84	0.73	0.59	0.91	0.58
	Parsa et al., [18]	-	-	-	0.31	0.1	-
	This work (CPC and MS model)	1.30	0.54	0.28	0.92	0.67	0.35
	This work (CPC and SS model)	1.76	1.06	0.58	1.15	0.91	0.67
	This work (SRK and MS model)	1.37	0.55	0.39	0.93	0.68	0.38
	This work (SRK and SS model)	1.83	1.08	0.59	1.18	0.93	0.71

4. Conclusion

In this study, multi-solid (MS) and solid solution (SS) thermodynamic model was developed using CPC EoS and tested for six ternary and binary systems. The results were next compared with previous models of n-Alkane mixtures. The results support the following conclusions:

The results showed that for these normal alkane systems, the accuracy of the CPC and SRK equations of state in obtaining the wax formation temperature is close to each other. Perhaps for systems containing heavier hydrocarbons, the CPC equation of state would provide better results.

The results of the multi-solid model were better in calculating the wax formation temperature for these normal alkane systems than the solid solution model. Moreover, the better results of multi-solid model can be possibly due to the consideration of the solid phase as an ideal solution in the solid solution model.

Also, evaluation against the literature indicated that the implemented model performed with similar precision compared with previously reported methodologies for these specific systems.

However, one of the limitations of the model is its application to heavy hydrocarbons. Determining the parameters of the CPC equation of state for heavy hydrocarbons is one of the limitations of

this model. It is proposed that this model can be used to calculate the wax formation temperature in real oil and gas systems. By developing the model and obtaining the model parameters, it can be extended to crude and dead oil and Fischer–Tropsch systems.

List of symboles

symbols	superscribes	subscribes
a: intermolecular attraction forces in Redlich- Kwong EoS	f : fusion property	c: critical property
b: co-volume	L: liquid phase	CPC: cubic plus chain
C_n: carbon number	S : solid phase	i, j: spices
C_p: heat capacity	SL: solid-liquid	pure: pure spices
f: fugacity	0 : standard state	sum: fusion plus solid state transition
$\hat{f}$: fugacity in mixture		tr: solid state transition
h: enthalpy		
k: equilibrium constant		
m: number of segments in the molecule		
MW: molecular weight		
P: pressure		
R: universal gas constant, 8.314 J mol^{-1} K^{-1}		
s: vector of solid phase mole fraction		
T: temperature		
x: vector of liquid phase mole fraction		
$\bar{m}$: average number of segments in the molecule for mixture		
$\bar{m}b$: CPC EoS parameter for mixture		
$\bar{m}^2 a$: CPC EoS parameter for mixture		
Greek letters:		
α : function of reduced temperature		
$\hat{\varphi}$: fugacity coefficient in mixture		
γ :activity coefficient in mixture		
Δ : difference		
Ω_a : constant of Redlich- Kwong EoS		
Ω_b : constant of Redlich- Kwong EoS		

References

[1] A. Firoozabadi, Thermodynamics of hydrocarbon reservoirs, (1999).

[2] H.P. Ronningsen, B. Bjorndal, A.B. Hansen, W.B. Pedersen, Wax precipitation from North Sea crude oils. 1. Crystallization and dissolution temperatures, and Newtonian and Non-Newtonian flow properties, Energy & Fuels, 5 (1991) 895-908.

[3] A. Hammami, M.A. Raines, Paraffin Deposition from Crude Oils: Comparison of Laboratory Results to Field Data, in: SPE Annual Technical Conference and Exhibition, 1997.

[4] H.-Y. Ji, B. Tohidi, A. Danesh, A.C. Todd, Wax phase equilibria: developing a thermodynamic model using a systematic approach, Fluid Phase Equilibria, 216 (2004) 201-217.

[5] J.M. Prausnitz, R.N. Lichtenthaler, E. Gomes de Azevedo, Molecular thermodynamics of fluid-phase equlibria, (1999).

[6] C. Lira-Galeana, A. Firoozabadi, J.M. Prausnitz, Thermodynamics of wax precipitation in petroleum mixtures, AICHE journal, 42 (1996) 239-248.

[7] K. Won, Thermodynamics for solid solution-liquid-vapor equilibria: wax phase formation from heavy hydrocarbon mixtures, Fluid Phase Equilibria, 30 (1986) 265-279.

[8] G. Soave, Equilibrium constants from a modified Redlich-Kwong equation of state, Chemical engineering science, 27 (1972) 1197-1203.

[9] K. Schou Pedersen, P. Skovborg, H.P. Roenningsen, Wax precipitation from North Sea crude oils. 4. Thermodynamic modeling, Energy & Fuels, 5 (1991) 924-932.

[10] J.A. Coutinho, E.H. Stenby, Predictive local composition models for solid/liquid equilibrium in n-alkane systems: Wilson equation for multicomponent systems, Industrial &

engineering chemistry research, 35 (1996) 918-925.
[11] J.A. Coutinho, K. Knudsen, S.I. Andersen, E.H. Stenby, A local composition model for paraffinic solid solutions, Chemical engineering science, 51 (1996) 3273-3282.
[12] J.A. Coutinho, Predictive UNIQUAC: a new model for the description of multiphase solid− liquid equilibria in complex hydrocarbon mixtures, Industrial & Engineering Chemistry Research, 37 (1998) 4870-4875.
[13] D.S. Abrams, J.M. Prausnitz, Statistical thermodynamics of liquid mixtures: a new expression for the excess Gibbs energy of partly or completely miscible systems, AIChE journal, 21 (1975) 116-128.
[14] D.-Y. Peng, D.B. Robinson, A new two-constant equation of state, Industrial & Engineering Chemistry Fundamentals, 15 (1976) 59-64.
[15] F. Esmaeilzadeh, J.F. Kaljahi, E. Ghanaei, Investigation of different activity coefficient models in thermodynamic modeling of wax precipitation, Fluid phase equilibria, 248 (2006) 7-18.
[16] S. Aftab, J. Javanmardi, K. Nasrifar, Experimental investigation and thermodynamic modeling of wax disappearance temperature for n-undecane+ n-hexadecane+ n-octadecane and n-tetradecane+ n-hexadecane+ n-octadecane ternary systems, Fluid Phase Equilibria, 403 (2015) 70-77.
[17] J. Gross, G. Sadowski, Perturbed-chain SAFT: An equation of state based on a perturbation theory for chain molecules, Industrial & engineering chemistry research, 40 (2001) 1244-1260.
[18] S. Parsa, J. Javanmardi, S. Aftab, K. Nasrifar, Experimental measurements and thermodynamic modeling ofwax disappearance temperature for the binary systems n-C14H30+ n-C16H34, n-C16H34+ n-C18H38 and n-C11H24+ n-C18H38, Fluid Phase Equilibria, 388 (2015) 93-99.
[19] K. Nasrifar, M.F. Kheshty, Effect of pressure on the solid–liquid equilibria of synthetic paraffin mixtures using predictive methods, Fluid phase equilibria, 310 (2011) 111-119.
[20] E. Ghanaei, F. Esmaeilzadeh, J. Fathikalajahi, Wax formation from paraffinic mixtures: A simplified thermodynamic model based on sensitivity analysis together with a new modified predictive UNIQUAC, Fuel, 99 (2012) 235-244.
[21] R. Bagherinia, M. Assareh, F. Feyzi, An improved thermodynamic model for Wax precipitation using a UNIQUAC+ PC-SAFT approach, Fluid Phase Equilibria, 425 (2016) 21-30.
[22] J. Yang, W. Wang, B. Shi, Q. Ma, P. Song, J. Gong, Prediction of wax precipitation with new modified regular solution model, Fluid Phase Equilibria, 423 (2016) 128-137.
[23] I.K. Nikolaidis, V.S. Samoili, E.C. Voutsas, I.G. Economou, Solid–Liquid–Gas Equilibrium of Methane–n-Alkane Binary Mixtures, Industrial & Engineering Chemistry Research, 57 (2018) 8566-8583.
[24] X. Wang, S. Li, H. Bai, C. Liu, New Predictive Nonrandom Two Liquid Equation for Solid–Liquid Phase Equilibrium in n-Alkanes Mixture with Multiple Solid Solutions, Industrial & Engineering Chemistry Research, 58 (2019) 18411-18421.
[25] F. Shariatrad, J. Javanmardi, A. Rasoolzadeh, A.H. Mohammadi, Experimental Measurement and Thermodynamic Modeling of the Wax Disappearance Temperature (WDT) for a Quaternary System of Normal Paraffins, ACS omega, 7 (2022) 16928-16938.
[26] D.V. Nichita, L. Goual, A. Firoozabadi, Wax precipitation in gas condensate mixtures, SPE Production & Facilities, 16 (2001) 250-259.
[27] R. Dalirsefat, F. Feyzi, A thermodynamic model for wax deposition phenomena, Fuel, 86 (2007) 1402-1408.
[28] F. Shaahmadi, M.A. Anbaz, B.H. Shahraki, Thermodynamic modeling of wax disappearance temperature in n-alkane mixtures by perturbed hard sphere chain equation of state, Fluid Phase Equilibria, 427 (2016) 557-565.
[29] Y. Song, T. Hino, S.M. Lambert, J.M. Prausnitz, Liquid-liquid equilibria for polymer solutions and blends, including copolymers, Fluid Phase Equilibria, 117 (1996) 69-76.
[30] M. Fermeglia, A. Bertucco, S. Bruni, A perturbed hard sphere chain equation of state for applications to hydrofluorocarbons, hydrocarbons and their mixtures, Chemical engineering science, 53 (1998) 3117-3128.
[31] B. Bazooyar, F. Shaahmadi, A. Jomekian, H.G. Darabkhani, Modelling of wax deposition by perturbed hard sphere chain equation of state, Journal of Petroleum Science and Engineering, 185 (2020) 106657.
[32] J.C.M. Escobar-Remolina, Prediction of characteristics of wax precipitation in synthetic mixtures and fluids of petroleum: A new model, Fluid Phase Equilibria, 240 (2006) 197-203.
[33] E.V. Asbaghi, M. Assareh, F. Nazari, An effective procedure for wax formation modeling using multi-solid approach and PC-SAFT EOS for petroleum fluids with PNA characterization, Journal of Petroleum Science and Engineering, 207 (2021) 109103.
[34] E.V. Asbaghi, F. Nazari, M. Assareh, M.M. Nezhad, Toward an efficient wax precipitation model: Application of multi-solid framework and PC-SAFT with focus on heavy end characterization for different crude types, Fuel, 310 (2022) 122205.
[35] A. Alhejaili, M.R.R.T. Goes, J. Howerton, N. Daraboina, Thermophysical properties of n-alkanes from C17 to C50 and validation of available correlations, Fluid Phase Equilibria, 583 (2024) 114106.
[36] B. Amiri-Ramsheh, M. Safaei-Farouji, A. Larestani, R. Zabihi, A. Hemmati-Sarapardeh, Modeling of wax disappearance temperature (WDT) using soft computing approaches: Tree-based models and hybrid models, Journal of Petroleum Science and Engineering, 208 (2022) 109774.
[37] M.N. Amar, N. Zeraibi, C. Benamara, H. Djema, R. Saifi, M. Gareche, Modeling wax disappearance temperature using robust white-box machine learning, Fuel, 376 (2024) 132703.
[38] M. Wang, C.-C. Chen, Predicting wax appearance temperature and precipitation profile of normal alkane systems: An explicit co-crystal model, Fluid Phase

Equilibria, 509 (2020) 112466.
[39] C.J. Sisco, M.I. Abutaqiya, F.M. Vargas, W.G. Chapman, Cubic-plus-chain (CPC). I: A statistical associating fluid theory-based chain modification to the cubic equation of state for large nonpolar molecules, Industrial & Engineering Chemistry Research, 58 (2019) 7341-7351.
[40] C.J. Sisco, M.I. Abutaqiya, F.M. Vargas, W.G. Chapman, Cubic-plus-chain (CPC). II: function behavior of the chain-modified cubic equation of state, Industrial & Engineering Chemistry Research, 58 (2019) 8810-8816.
[41] M. Mansourpoor, R. Azin, S. Osfouri, A. Izadpanah, Experimental measurement and modeling study for estimation of wax disappearance temperature, Journal of Dispersion Science and Technology, 40 (2019) 161-170.

Appendix A: Cubic plus chain equation of state

$m_0=\frac{1-m}{m}$	(A-1)
$c_0=-128000-128000\,m_0$	(A-2)
$c_1=566400+566400\,m_0$	(A-3)
$c_2=-249840-748800\,m_0$	(A-4)
$c_3=-145562+188800\,m_0$	(A-5)
$c_4=36366+182400\,m_0$	(A-6)
$c_5=45486$	(A-7)
$c_6=-13718-60800\,m_0$	(A-8)
$c_6\beta_c^6+c_5\beta_c^5+c_4\beta_c^4+c_3\beta_c^3+c_2\beta_c^2+c_1\beta_c+c_0=0$	(A-9)
$\lambda^{mon}=-\beta_c\frac{\beta_c^2+2\beta_c-1}{\left(1+\beta_c\right)^2}$	(A-10)
$\lambda^{chain}=-\beta_c\frac{840\beta_c}{\left(40-19\beta_c\right)^2}$	(A-11)
$Z_c^{mon}=\frac{1}{\left(1-\beta_c\right)}\left(1+\frac{\beta_c}{\lambda^{mon}\left(1+\beta_c\right)}\right)^{-1}$	(A-12)
$Z_c^{chain}=\left(\frac{\beta_c}{\left(1+\beta_c\right)}\frac{\lambda^{chain}}{\lambda^{mon}}+\frac{40}{40-19\beta_c}\right)\left(1+\frac{\beta_c}{\lambda^{mon}\left(1+\beta_c\right)}\right)^{-1}$	(A-13)
$Z_c=m\,Z_c^{mon}-\left(m-1\right)Z_c^{chain}$	(A-14)
$\Omega_a\left(m\right)=\frac{1}{m^2}\left(\frac{\beta_c Z_c^2}{\lambda^{mon}}+\left(m-1\right)\beta_c\frac{Z_c\lambda^{chain}}{\lambda^{mon}}\right)$	(A-15)
$\Omega_b\left(m\right)=\frac{1}{m}\beta_c Z_c$	(A-16)
$\alpha=\sqrt{\frac{T_c}{T}}$	(A-17)
$a_i=\Omega_{a_i}\left(m_i\right)\frac{R^2T_{c,i}^2}{P_{c,i}}\alpha$	(A-18)

$b_i = \Omega_{b_i}\left(m_i\right)\frac{RT_{c,i}}{P_{c,i}}$	(A-19)
$\overline{m} = \sum_{i=1}^{c} x_i\, m_i$	(A-20)
$\overline{m}\, b = \sum_{i=1}^{c} x_i\, m_i\, b_i$	(A-21)
$a_{ij} = \sqrt{a_i\, a_j}\left(1-k_{ij}\right)$	(A-22)
$\overline{m}^2\, a = \sum_{i=1}^{c}\sum_{j=1}^{c} x_i\, x_j\, m_i\, m_j\, a_{ij}$	(A-23)
$P_{CPC} = \frac{RT}{\upsilon}\left(1+\frac{\overline{m}\left(\overline{m}\, b\right)}{\upsilon-\overline{m}\, b}\right) - \frac{\overline{m}^2 a}{\upsilon\left(\upsilon+\overline{m}\, b\right)} - \frac{RT}{\upsilon}\left(\frac{\overline{m}\, b}{\upsilon}\sum_{i=1}^{c} x_i\left(m_i-1\right)\frac{0.475\upsilon}{\upsilon-0.475\overline{m}\, b}\right)$	(A-24)
$g = \frac{\upsilon}{\upsilon-0.475\overline{m}\, b} = \frac{1}{1-0.475\frac{\overline{m}\, b}{\upsilon}} = \frac{1}{1-0.475\beta}$	(A-25)
$\beta = \frac{\overline{m}\, b}{\upsilon}$	(A-26)
$\frac{A^R}{nRT} = \frac{a^R}{RT} = m\frac{a^{mono,R}}{RT} + \frac{a^{chain,R}}{RT}$	(A-27)
$\frac{a^R}{RT} = -\overline{m}\ln\left(1-\beta\right) - \frac{\overline{m}^2 a}{\left(\overline{m}b\right)RT}\ln\left(1+\beta\right) - \sum_{i=1}^{c} x_i\left(m_i-1\right)\ln\left(g\right)$	(A-28)

نشریه فناوری نفت، گاز و پتروشیمی، ۱۲(۱): ۱-۱۷، زمستان و بهار ۱۴۰۴

مقاله تحقیقاتی

مدلسازی ترمودینامیکی دمای تشکیل واکس در سامانه‌های پارافینی با استفاده از معادله حالت مکعبی به اضافه زنجیره

رامین جمالی، امیر عباس ایزدپناه*، حسین رهیده

گروه مهندسی شیمی، دانشکده مهندسی نفت، گاز و پتروشیمی، دانشگاه خلیج فارس، بوشهر، صندوق پستی ۷۵۱۶۹۱۳۸۱۷، ایران

مشخصات مقاله

تاریخچه مقاله:

دریافت: ۷ آذر ۱۴۰۳

دریافت پس از اصلاح: ۳۰ اسفند ۱۴۰۳

پذیرش نهایی: ۳ فروردین ۱۴۰۴

کلمات کلیدی:

معادله حالت مکعبی به اضافه زنجیره

دمای تشکیل واکس

جامد چندگانه

محلول جامد

*عهده‌دار مکاتبات: امیر عباس ایزدپناه

رایانامه: izadpanah@pgu.ac.ir

تلفن: ۰۷۷-۳۱۲۲-۲۶۰۷

چکیده

هدف از این پژوهش توسعه یک مدل ترمودینامیکی برای پیش بینی دمای تشکیل واکس با استفاده از معادله حالت مکعبی به اضافه زنجیره (CPC) و مدل‌های محلول جامد و جامد چندگانه است. سامانه های استفاده شده در این کار سامانه های دوتایی و سه تایی از نرمال آلکان‌ها می باشند. در مدل محلول جامد، فاز جامد به صورت محلول ایده‌آل در نظر گرفته شده است. در این تحقیق، نتایج مدلسازی دمای تشکیل واکس برای شش سامانه هیدروکربنی به دست امده است و با نتایج تجربی مقایسه شده است. سامانه های هیدروکربنی شامل سه سامانه سه جزئی شامل C14-C15-C16، C16-C17-C18 و C19-C20-C18 و همچنین سه سامانه دوجزئی شامل C14-C16، C17-C19 و C16-C18 می باشند. با توجه به نتایج به دست آمده، خطای متوسط مطلق در محاسبه دمای تشکیل واکس برای این سامانه ها ۱/۰۳٪ برای مدل محلول جامد و ۰/۶۷٪ برای مدل جامد چندگانه بود. با توجه به خطای متوسط مطلق برای این سامانه ها، مشاهده می‌شود که مدل جامد چندگانه نسبت به مدل محلول جامد نتایج بهتری ارایه داده است. با مقایسه نتایج به دست آمده با استفاده از معادلات حالت مکعبی به اضافه زنجیره و سوآو-ردلیچ-کوانگ (KRS) مشخص شد که نتایج این دو معادله حالت برای این نرمال آلکان‌ها تقریباً شبیه هم می باشد. مقایسه نتایج به دست آمده در این کار با کارهای پارسا و همکاران، غنایی و همکاران، شاه احمدی و همکاران و منصورپور و همکاران نشان داد که دقت مدل استفاده در این تحقیق قابل مقایسه و قابل توجه در نسبت به این مدل‌ها می باشد و نسبت به بعضی از این مدل‌ها نتایج بهتری ارایه می کند

نحوه استناد به این مقاله:

Jamali R, Izadpanah AA, Hossein Rahideh H., Thermodynamic Modeling of Wax Formation Temperature in Paraffinic Systems Using Cubic Plus Chain Equation of State, Journal of Oil, Gas and Petrochemical Technology, 2025; 12(1): 43-17. DOI:10.22034/jogpt.2025.490790.1132.